



OPEN

Joint analysis of structured and semi-structured community science data improves precision of relative abundance but not trends in birds

Alexander R. Schindler^{1,2}✉, Stephanie A. Cunningham³, Toryn L. J. Schafer⁴, Emily A. Sinnott², Sarah J. Clements², Frances M. DiDonato², Alisha R. Mosloff², Clay M. Walters^{1,2}, Amy A. Shipley², Mitch D. Weegman^{1,2} & Qing Zhao^{2,5}

Estimating absolute and relative abundance of wildlife populations is critical to addressing ecological questions and conservation needs, yet obtaining reliable estimates can be challenging because surveys are often limited spatially or temporally. Community science (i.e., citizen science) provides opportunities for semi-structured data collected by the public (e.g., eBird) to improve capacity of relative abundance estimation by complementing structured survey data collected by trained observers (e.g., North American breeding bird survey [BBS]). We developed two state-space models to estimate relative abundance and population trends: one using BBS data and the other jointly analyzing BBS and eBird data. We applied these models to seven bird species with diverse life history characteristics. Joint analysis of eBird and BBS data improved precision of mean and year-specific relative abundance estimates for all species, but the BBS-only model produced more precise trend estimates compared to the joint model for most species. The relative abundance estimates of the joint model were particularly more precise than the BBS-only estimates in areas where species detectability was low resulting from either low BBS survey effort or low abundance. These results suggest that community science data can be a valuable resource for cost-effective improvement in wildlife abundance estimation.

Understanding spatial and temporal variation in wildlife abundance is a fundamental question in population and community ecology. Estimating abundance is challenging, however, as surveys cannot cover all areas and animals cannot be counted with perfect detection. Survey data based on a structured sampling design allows practitioners to quantify observation error and thus make reasonable inference despite imperfect detection, but such surveys are often limited in spatial extent because of financial or logistical constraints. Community science (i.e., citizen science, public participation in scientific research) data collected by volunteer observers has emerged as an essential resource to address such limitations and fill crucial information gaps in monitoring, conservation, and ecological research^{1,2}. Community science data can provide information at larger scales not feasible with traditional structured surveys and increase public engagement in conservation³, but also has shortcomings such as uneven sampling over time and space, uneven sampling effort per visit, and variability in volunteer abilities to detect different species⁴. Participation in community science programs has increased steadily³ along with development of new analytical techniques that increase the utility of data collected for informing conservation efforts (e.g. Refs.^{5,6}).

Data integration has increasingly been used to improve estimation and inference capacity through joint analysis of separate but complementary data⁷. Integrated models share parameters between component sub-models

¹Department of Biology, University of Saskatchewan, Saskatoon, SK, Canada. ²School of Natural Resources, University of Missouri, Columbia, MO, USA. ³Department of Environmental Biology, State University of New York College of Environmental Science and Forestry, Syracuse, NY, USA. ⁴Department of Statistics and Data Science, Cornell University, Ithaca, NY, USA. ⁵Bird Conservancy of the Rockies, Fort Collins, CO, USA. ✉email: alexschindler@gmail.com

to overcome potential parameter estimate biases and missing information present in individual datasets⁴. For example, presence-absence data can be combined with presence-only data for improved models of species distribution⁸. Integrating community science data with other structured data sources could improve insight about ecological patterns and processes^{9,10}.

A wealth of bird-specific structured survey data is readily available and accessible to scientists and conservation practitioners. One of the most extensive of these datasets is the North American Breeding Bird Survey (BBS)¹¹. BBS is a long-term, international monitoring program of North American bird species conducted by the U.S. Geological Survey and Canadian Wildlife Service that has been running annually during peak bird breeding (May and June) since 1966. BBS data can be used to estimate relative abundance while accounting for observation error because these data follow a standardized protocol¹². BBS data are commonly used to study population trends and species distributions^{13,14}, yet observer availability and restriction to roads may lead to spatially unequal sampling and limited representation of some habitat types and species^{15–18}.

Semi-structured data, on the other hand, often cover a larger spatial extent than structured surveys, but generally lack aspects of rigorous protocols¹⁹ (e.g., trained observers, structured routes, etc.). eBird is one of the largest community science projects in North America. It is maintained by the Cornell Lab of Ornithology and National Audubon Society and allows observers to contribute observations to a publicly available database²⁰. As of 2020, 915 million bird sightings had been uploaded to eBird and over 400 peer-reviewed scientific papers had been published making use of these data (<https://ebird.org>). eBird data have been used to quantify population trends²¹, species distributions²², and relative abundance²³. Yet the semi-structured nature of eBird observations can present challenges to analyzing and interpreting data. Participants preferentially record some species over others (unequal taxonomic sampling), and observations are most common near populated or easy-to-access areas, on weekends, or during migration events (spatially and temporally unequal sampling), and there are often large discrepancies between number of detections and non-detections. However, data filtering practices can substantially reduce these^{24,25}.

While it is difficult to estimate relative abundance using eBird alone, both BBS and eBird data can provide strong estimates of population trends^{13,14}. Several studies have used eBird and BBS data to quantify species distributions using hierarchical models. Dorazio²⁶ developed a species distribution model to jointly analyze planned survey data and opportunistic presence-only data which reduced biases in environmental covariate estimates obtained from models using presence-only data alone. Pacifici et al.²⁷ found a joint analysis of eBird and BBS data improved occupancy estimates and predicted species distributions of brown-headed nuthatches (*Sitta pusilla*), compared to analyses using eBird data alone. A joint analysis of relative abundance using BBS and eBird data leveraging strengths of each dataset has the potential to improve the value and precision of range-wide relative abundance and trend estimates²⁸, yet such an approach has not been developed or evaluated.

In this study, we developed two models to estimate relative abundance and population trends in 1-degree grid cells across bird species ranges in North America: one using only BBS data (hereafter BBS model) and the other jointly analyzing BBS and eBird data (hereafter joint model). Differences in species life histories or other characteristics (e.g., spatial extent of distributions, density) can affect strength of inference from population models²⁹. For example, population trends may be predicted more accurately with eBird and BBS for species with broader spatial and elevational ranges¹³. We evaluated differences in the precision of relative abundance and population trend estimates between BBS-only and joint models within and among bird species in five orders and six families representing a variety of morphologies, life history characteristics, and distributions, likely relating to different detection potential. We expected precision of relative abundance and population trends would be generally improved in joint models relative to BBS-only models. We then examined spatial variation in relative abundance and trend estimates from BBS-only and joint models and anticipated that improvements in precision would be greatest in areas of low relative abundance or at the periphery of a species distribution.

We assessed the relative abundance and population trend estimates of the BBS-only and joint models for a suite of species, as the extent to which migration strategy, habitat preference, and/or population trend influences estimate of relative abundance has not been evaluated: American woodcock (*Scolopax minor*), black-billed cuckoo (*Coccyzus erythrophthalmus*), black-throated blue warbler (*Setophaga caerulescens*), Canada goose (*Branta canadensis*), loggerhead shrike (*Lanius ludovicianus*), northern bobwhite (*Colinus virginianus*) and upland sandpiper (*Bartramia longicauda*). American woodcock, black-billed cuckoo, black-throated blue warbler, Canada goose and upland sandpiper are migratory birds^{30–34}, loggerhead shrike are partial migrants³⁵ and northern bobwhite are non-migratory³⁶. These species have diverse habitat preferences including interior forest, forest opening/edge, open grassland, and wetland^{30–36}, which may result in variation in detectability. We anticipated that relative abundance estimates for less detectable species (e.g., those rare or cryptic, inhabiting dense forest habitat) would have greatest improvement in precision with additional data relative to more detectable species (e.g., common species, inhabiting open habitat easily seen from a road). We further anticipated that precision in trend estimates would increase for species that are detected less frequently or have greater variability in detection rates³⁷. We evaluated precision in relative abundance and trend estimates from BBS-only and joint models within and among species using the coefficient of variation (CV; see “Methods” section).

Results

Estimated mean relative abundance (α) per grid cell was similar within species between BBS-only and joint models (Fig. 1). Generally, the relative abundance indices had high frequency of low to moderate relative abundance (i.e., the distribution peaked at low densities of birds; Fig. 1), except for Canada goose, whose BBS abundance peaked at a relatively large abundance per grid cell, but also had moderate frequency of low to moderate relative abundance. The American woodcock BBS and joint models would not converge (i.e., $\hat{R} > 1.2$ and chains did not mix). The model converged only when we added an additional data type (i.e., Singing Ground Survey [SGS]).

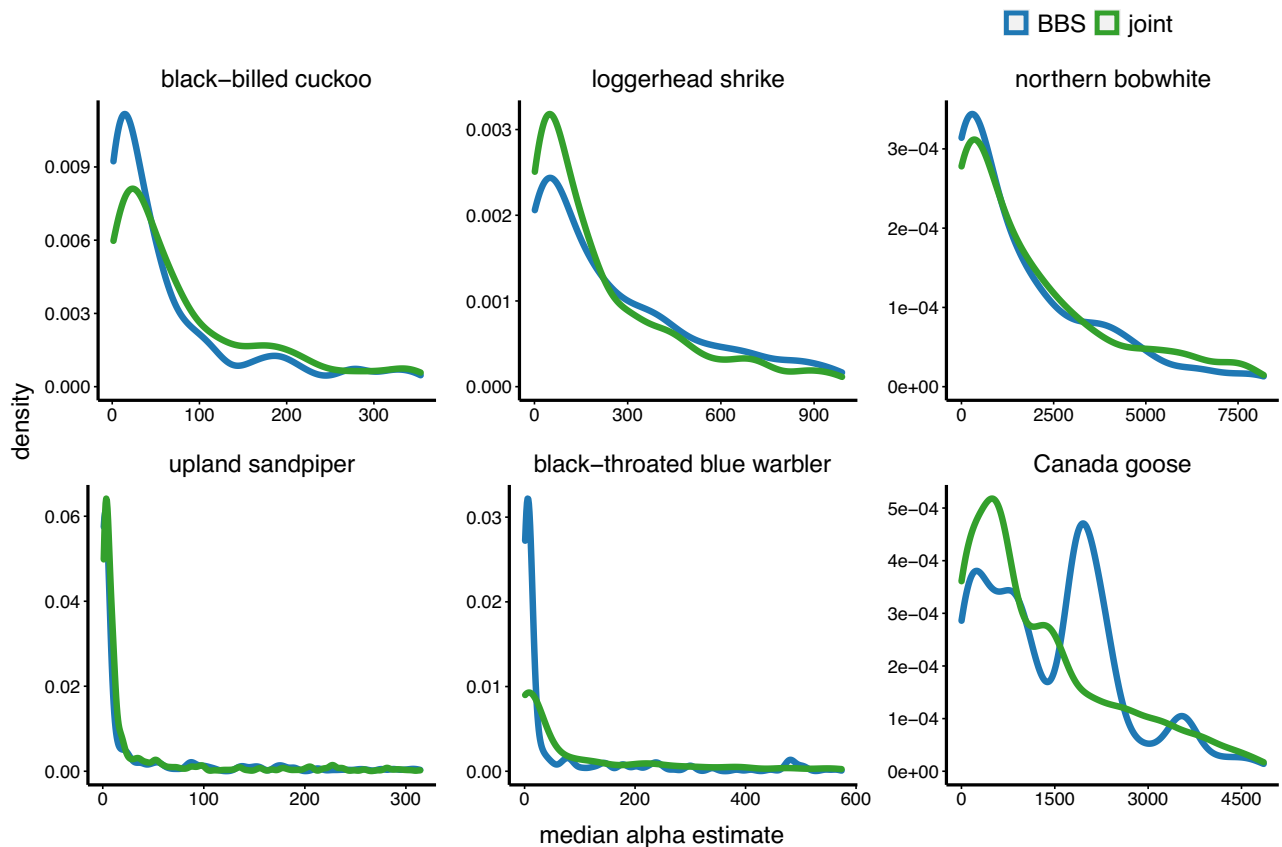


Figure 1. Distribution of per-grid cell relative abundance estimates across respective study areas for BBS only and joint models for black-billed cuckoo, loggerhead shrike, northern bobwhite, upland sandpiper, black-throated blue warbler, and Canada goose. The x-axis represents the range of per-grid cell estimates of mean relative abundance (α) from the respective models and the y-axis represents the density of the respective α estimates among all grid cells (i.e., the relative frequency of grid cells with the respective relative abundance).

Mean (α) as well as year-specific (γ) relative abundance estimates for all species were more precise from the joint model relative to the BBS model (i.e., > 50% of grid cells had lower CV from the joint model relative to CV from the BBS model). The proportion of grid cells with lower CV for the joint model relative to the BBS model for mean and year-specific relative abundances were 0.98 and 0.99 for black-billed cuckoo, 0.93 and 0.93 for northern bobwhite, 0.92 and 0.88 for loggerhead shrike, 0.78 and 0.90 for upland sandpiper, 0.64 and 0.79 for black-throated blue warbler, and 0.58 and 0.84 for Canada goose, respectively. Thus, among species, precision across grid cells was least improved in the mean relative abundances of Canada goose and black-throated blue warbler.

Mean relative abundance CV differences between BBS-only and joint models were greatest (i.e., lowest joint model CVs relative to BBS-only model CVs) for black-billed cuckoo, loggerhead shrike, and northern bobwhite for grid cells with lowest relative abundances and least (i.e., highest joint model CVs relative to BBS-only model CVs) for grid cells with highest relative abundances, as hypothesized. In other words, greatest improvements in precision using the joint model instead of the BBS-only model were realized under lowest estimated mean relative abundances for these species (Figs. 2, 3, 4, Fig. S2). Mean relative abundance CV differences for upland sandpiper also generally followed this pattern, except for grid cells in the 25th to 50th percentile, where gain in precision exceeded that below the 25th percentile (Fig. 2, Fig. S3). Mean relative abundance CV differences for black-throated blue warbler and Canada goose increased with relative abundance whereby greatest improvements in precision between BBS-only and joint models occurred in grid cells with highest relative abundances (Fig. 2, Figs. S4, S5). There were no substantial patterns in the mean relative abundance CV differences for distance to edge of range; precision in relative abundance estimates did not markedly improve in the joint model at greatest distances to edge from species distribution centroid (Fig. S6).

Mean relative abundance CV differences between BBS-only and joint models for black-billed cuckoo, loggerhead shrike, northern bobwhite, and upland sandpiper were greatest in grid cells with fewest BBS routes (Fig. S8). For these species, precision was most improved in the joint model relative to the BBS-only model in grid cells with few BBS routes. However, for black-throated blue warbler and Canada goose, mean relative abundance CV differences between BBS-only and joint were greatest in grid cells with greatest number of BBS routes (Fig. S8). Mean relative abundance CV differences between BBS-only and joint models were greatest in grid cells with fewest eBird checklists for upland sandpiper, but greatest in grid cells with greatest number of eBird checklists for black-throated blue warbler and Canada goose. There were no substantial patterns in mean relative abundance CV improvements with number of eBird checklists for the other species (Fig. S10).

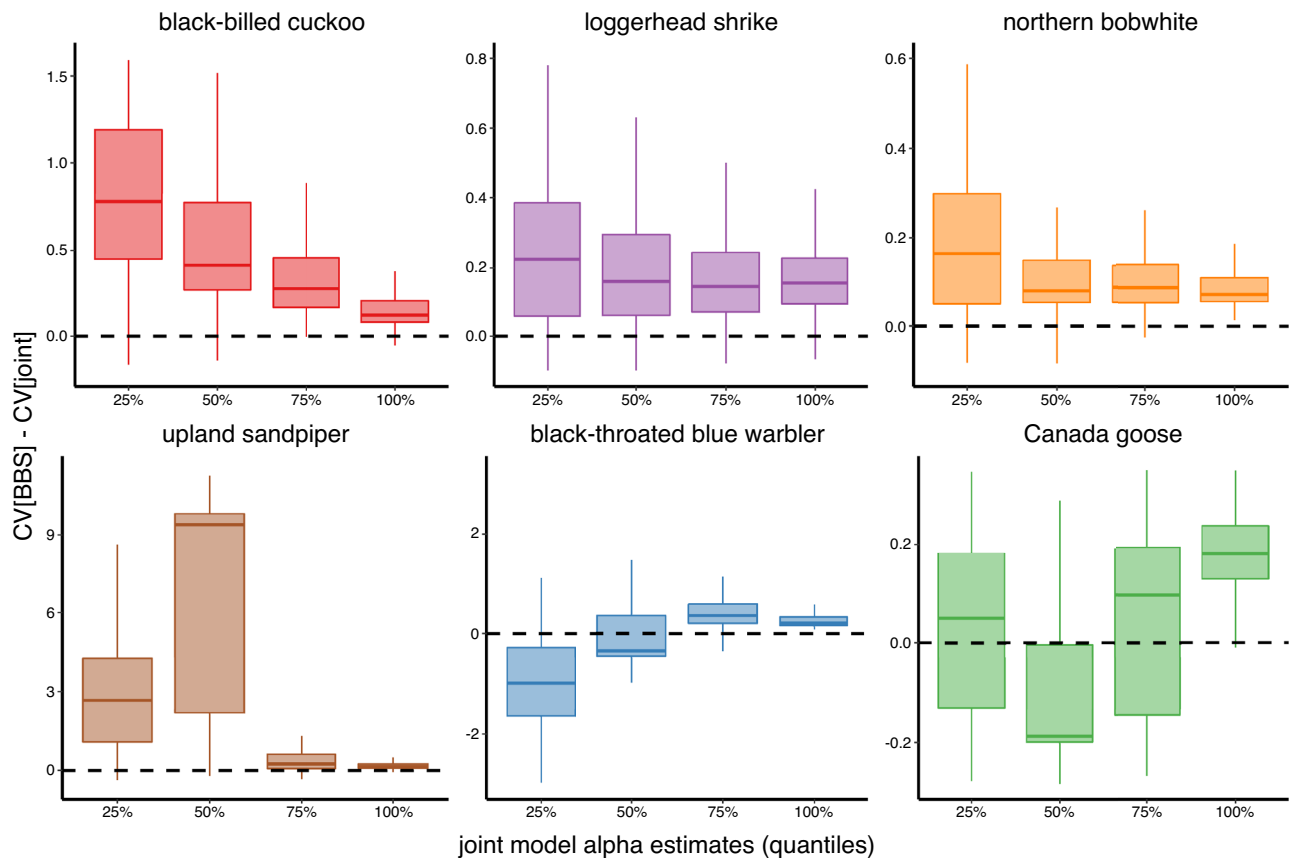


Figure 2. Improvements in precision (i.e., $CV[BBS\ model] - CV[joint\ model]$) of mean relative abundance (α) estimates for each grid cell in response to corresponding black-billed cuckoo, loggerhead shrike, northern bobwhite, upland sandpiper, black-throated blue warbler, and Canada goose relative abundances. Relative abundance values on the x-axis represent joint model α estimates and are depicted as 25 percentile ranges. Values above the dashed line indicate that estimates from a joint model were more precise than those from a BBS model, whereas values below that indicate that estimates from a joint model were less precise.

Trend (β) estimates for black-billed cuckoo and Canada goose were more precise in the joint model relative to the BBS model (proportion of grid cells where joint model CV was lower = 0.68 and 1.00, respectively). Trend estimates for most grid cells for all other species were more precise in the BBS model relative to the joint model. Trend estimates for northern bobwhites were more precise in the joint model relative to the BBS model (i.e., joint model CVs were lower than BBS-only model CVs) in some grid cells with low relative abundance, in the core area of the range (i.e., smallest distance to edge), or with few BBS routes (Figs. 4, 5, Figs. S7, S9). Trend estimates for black-throated blue warbler were more precise in the joint model relative to the BBS model in some grid cells with many eBird checklists (Fig. S11). The number of BBS routes and eBird checklists were strongly correlated only for black-throated blue warbler and Canada goose (i.e., $r \sim 0.68$; Fig. S12).

Discussion

Information about spatiotemporal variation in abundance is crucial for conservation planning and management of wildlife species. We developed models that jointly analyzed North American Breeding Bird Survey (BBS) and eBird data, using bird species representing a variety of life histories, which estimated spatially explicit indices of mean relative abundance across study years (α), indices of year-specific relative abundance (γ), and trends in relative abundance indices (β) from 2010 to 2019. Mean and year-specific relative abundance estimates from joint models were more precise than those from BBS models for most grid cells for six of the seven species we studied. In the case of our seventh study species, American woodcock, data integration allowed us to estimate relative abundance and trends when we could not do so with one dataset alone. While BBS and eBird data only allow us to estimate an index of relative abundance and not actual abundance at the grid cell level, such indices are a useful tool for conservation practitioners^{38–40}. Overall, our modeling framework will allow conservation practitioners to integrate count data collected on different spatiotemporal scales and identify areas that have averaged high densities of a species over time (i.e., high α values), high density areas in a particular year (i.e., high γ values), and areas where relative abundance is increasing or decreasing (i.e., positive or negative β values, respectively).

As anticipated, CV difference in mean relative abundance was greater when relative abundance was lower, and greatest improvement in CV was generally associated with fewer BBS routes for black-billed cuckoo, loggerhead shrike, northern bobwhite and upland sandpiper. Thus, relative abundance estimates were more precise

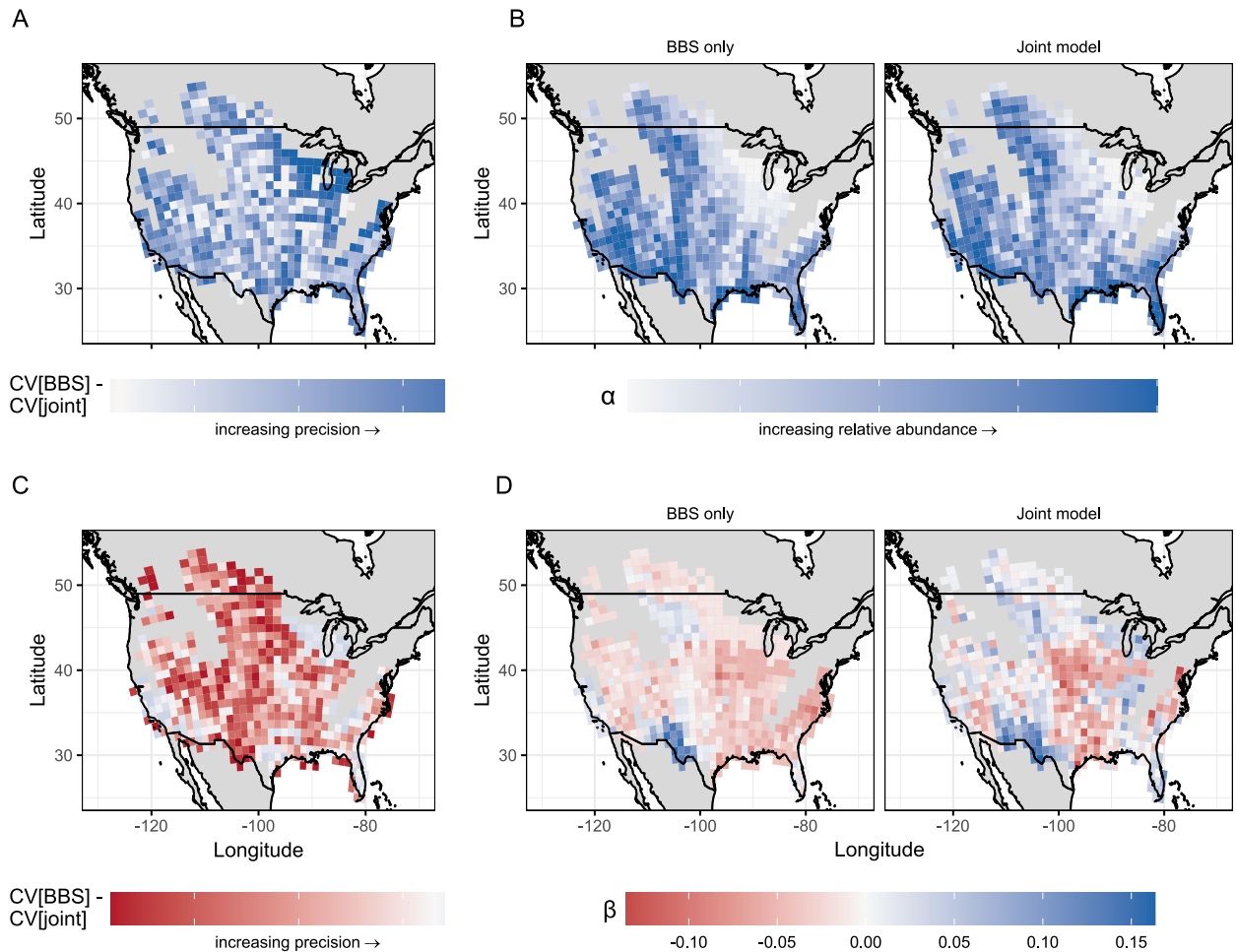


Figure 3. Comparison of precision (i.e., $CV[BBS]-CV[joint]$); (A,C) between BBS-only and joint models for relative abundance (α ; top row) and trend (β ; bottom row) of loggerhead shrike. Model-specific estimates of mean relative abundance in are shown in (B), and estimates of mean trend in (D). In all panels, blue indicates a positive value/increase and red a negative value or decrease, while 0 is set to white.

after adding eBird data when there were fewer detections resulting from either low BBS survey effort or low relative abundance of these species. However, we found the opposite patterns in CV difference in mean relative abundance for black-throated blue warbler and Canada goose (i.e., greatest CV difference occurred at greatest mean relative abundance). For Canada goose, we believe this is a result of limited BBS and eBird data in the northern part of the species range (i.e., BCRs 1–7; Supplementary Information Fig. S13), which contain large areas of temperate or boreal forest, or tundra, with low densities of people. Such conditions impede access by both community scientists and BBS observers^{41,42}. We therefore recommend caution when interpreting relative abundance and trend estimates in these areas where survey data are limited. In the case of black-throated blue warbler, the lack of improvement in precision when integrating several data types may be due to black-throated blue warbler habitat use, which may influence detectability in eBird observations and BBS surveys. Black-throated blue warblers are most likely to occur in unfragmented tracts of forest of at least 100 ha and therefore less likely to be detected than species occupying open, more accessible areas regardless of survey type^{43–45}. Because the species is both area-dependent and occupies habitats with dense forests and shrubs during the breeding season³², it is likely that roadside BBS surveys are less likely to detect it than other species in our study, which occupy open (loggerhead shrike, northern bobwhite, upland sandpiper, Canada goose^{33–36}) or forest edge (black-billed cuckoo³¹) habitats. Adding eBird data may only improve precision for areas in which area-dependent species are abundant enough to be easily detected by observers.

Life history differences likely further affected improvements between joint and BBS-only models. Precision in black-billed cuckoo abundance was most improved in joint vs. BBS-only models, while Canada goose abundance estimates were least improved. Black-billed cuckoos are sit-and-wait predators and are generally patchily distributed, making them difficult to detect with traditional point-count surveys^{31,46}. In contrast, Canada geese favor open area habitats and are easily detected³³. Integrating eBird data may therefore be especially beneficial for less detectable (e.g., less vocal or conspicuous) species. However, we acknowledge our seven focal species represent a small sample size and encourage further research to examine how life history differences affect improvements

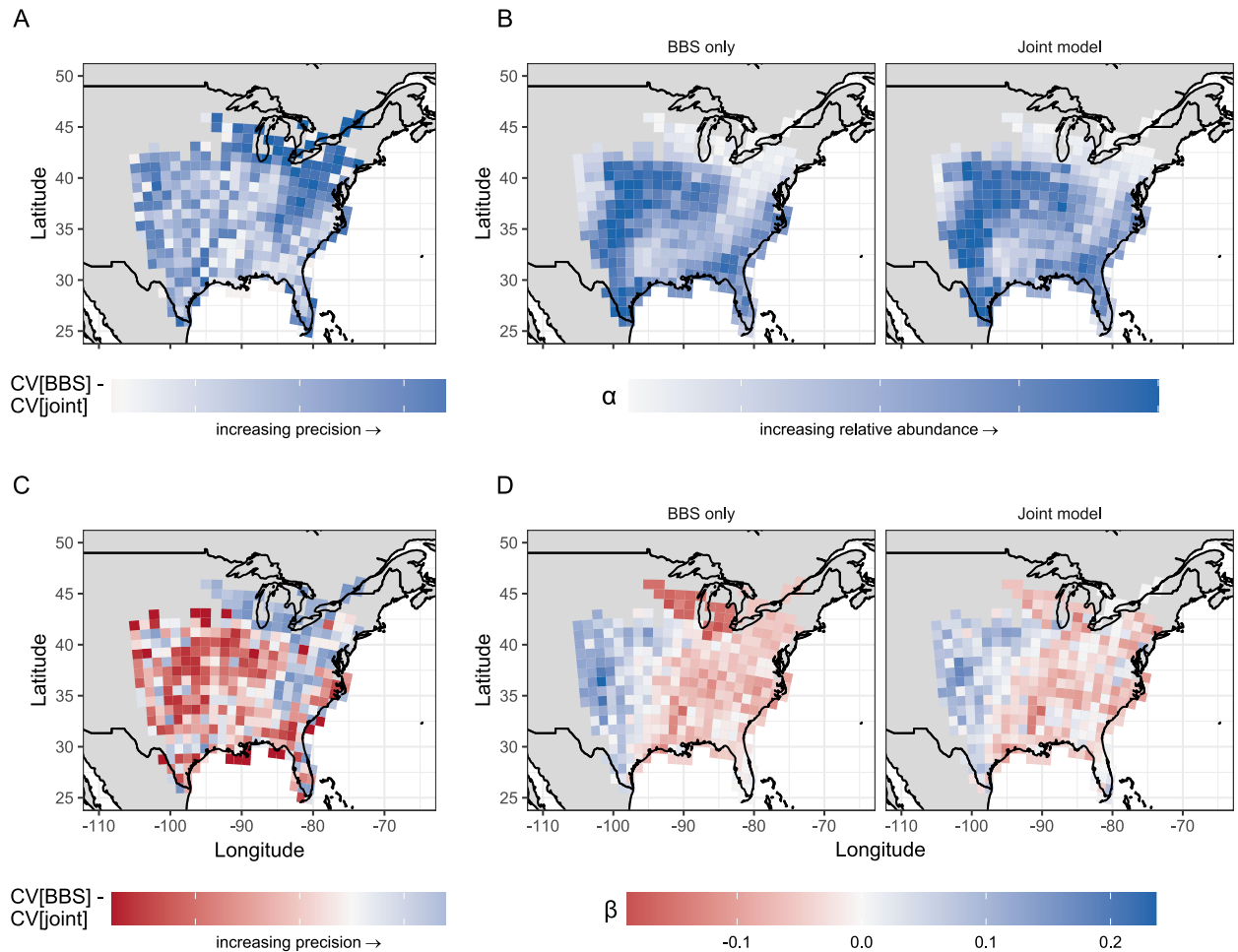


Figure 4. Comparison of precision (i.e., $CV[BBS] - CV[joint]$); (A,C) between BBS-only and joint models for relative abundance (α ; top row) and trend (β ; bottom row) of northern bobwhite. Model-specific estimates of mean relative abundance in are shown in (B), and estimates of mean trend in (D). In all panels, blue indicates a positive value/increase and red a negative value or decrease, while 0 is set to white.

in abundance estimates from data integration. The American woodcock models required a third dataset, the Singing-Ground Survey, to converge. American woodcocks are most detectable in the evening when males exhibit courtship behavior³⁰, and detection rates of American woodcocks during the BBS and other standard morning point-count surveys are generally low⁴⁷. While we expected integrating eBird data in American woodcock models would improve parameter estimation, the number of American woodcock detections in eBird data may not have been sufficient without additional data from the Singing Ground Survey, which was designed to maximize detection probability of this species.

Contrary to our hypotheses, our trend estimates were more precise for BBS models compared to models with multiple data types for all species except black-billed cuckoo and Canada goose. In some cases, the joint model estimates indicated an increasing trend where the BBS-only model indicated a declining trend (e.g. Fig. 3, Figs. S2–S4). To illustrate our data integration approach, we structured our models to estimate a simple linear trend in abundance over our study period. Although we used a relatively short time series of data (10 years), we anticipate abundance of many of these species may not have increased or decreased linearly over time. In cases where abundance did not change linearly (e.g., increased for a few years before decreasing, decreased for a few years before decreasing less severely, etc.), increased precision in our relative abundance estimates may have increased uncertainty in our linear trend estimate (i.e., we may have been less likely to detect a linear trend where a linear trend did not exist). In such cases, our BBS model trend estimates may have been overly precise. A modeling framework with the flexibility to estimate nonlinear trends may be more appropriate and yield more accurate trend estimates. We encourage more research to evaluate the tradeoffs between increased precision in abundance and decreased precision in trend estimates.

We anticipated improvements in precision of trend estimates would be greatest in areas of low relative abundance (i.e., adding more data would improve precision in estimates where abundance was low, and birds were therefore less detectable). However, the relationship between trend precision and relative abundance was variable between species. For example, we observed increased precision in mean trend estimates for black-billed cuckoo

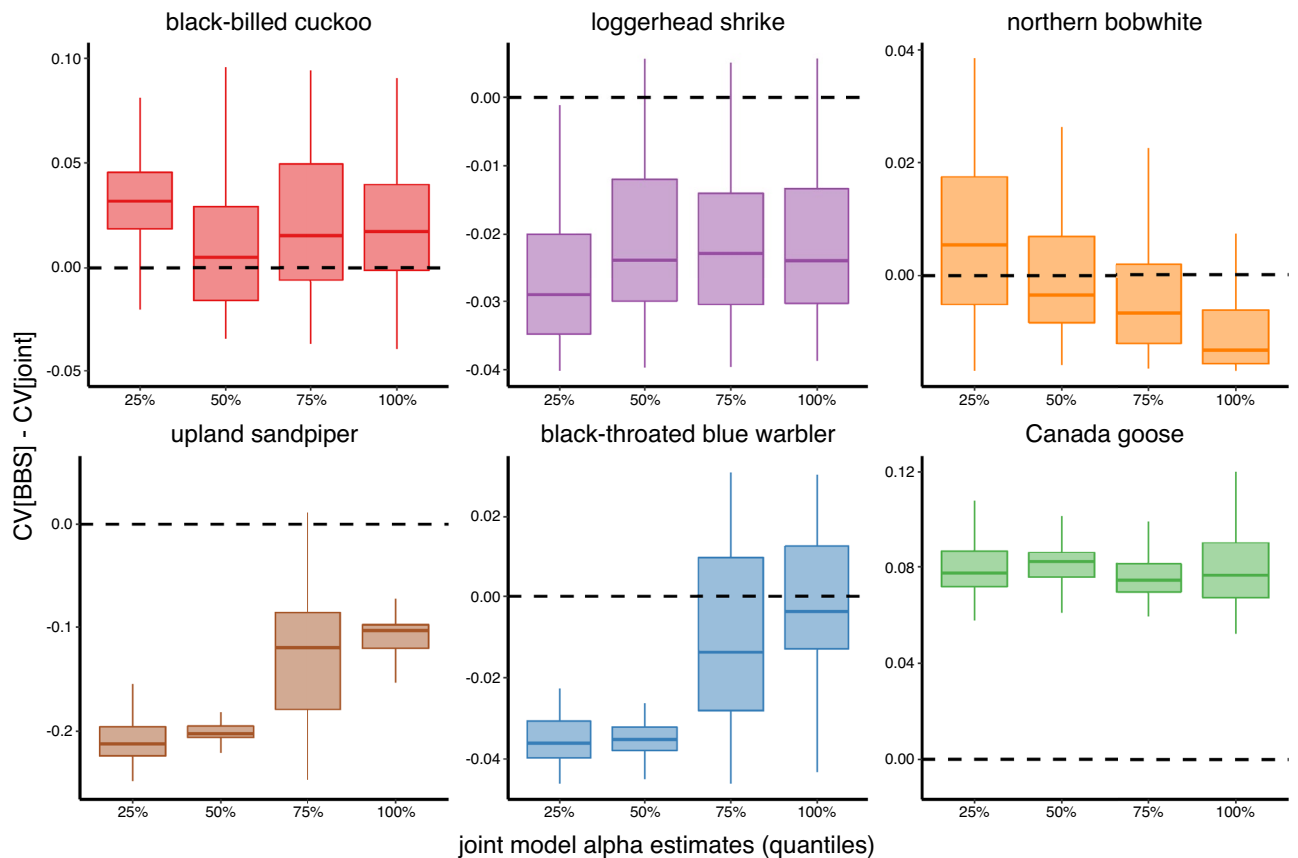


Figure 5. Improvements in precision (i.e., $CV[BBS \text{ model}] - CV[\text{joint}]$) of trend (β) estimates for each grid cell in response to corresponding black-billed cuckoo, loggerhead shrike, northern bobwhite, upland sandpiper, black-throated blue warbler, and Canada goose relative abundances. Relative abundance values on the x-axis represent joint model α estimates and are depicted as 25 percentile ranges. Values above the dashed line indicate that estimates from a joint model were more precise than those from a BBS model, whereas values below that indicate that estimates from a joint model were less precise.

along the western edge of their range, which had lower estimates for relative abundance, whereas the joint model did not improve precision of trend estimates for some of the grid cells with the highest estimates of relative abundance (in the northern part of the species' range; Fig. S2). However, in black-throated blue warblers, the areas of greatest relative abundance appeared to have the highest precision in trend estimates (Fig. S4).

Theoretical and empirical work has indicated that abundance of species decreases with increasing distance from center of range, or more accurately, center of niche^{48,49}. Therefore, we expected lower relative abundances of birds at the edge of their ranges, and that precision of our joint model would be greater in grid cells on range peripheries. However, we did not find such patterns in any species we examined, and there was little difference in precision between cells at the periphery of range and those in the center (Fig. S6). We anticipate that this may be due, in part, to our calculation of the geographic center rather than niche center, as well as the coarse resolution (12,321 km²) of grid cells⁵⁰ and species' range definitions (i.e., including whole BCRs if any portion of the BCR contained detections of the species), which might not capture sharp declines in relative abundance if they occur over a relatively small distance⁵¹. Further, strength of relationship may vary by species, according to traits such as body size, niche-breadth, and distribution of species relative to their available niche^{48,50}. We suggest practitioners further explore these finer scale applications of our approach to more deeply understand how precision may be improved at range edges.

Locations of surveys and checklists in the BBS and eBird datasets, respectively, are non-random and limited to road proximity (in the case of BBS surveys) and human activity (in the case of eBird surveys), which can lead to biased abundance and trend estimates⁵². We incorporated an observer-by-route error term ($\epsilon_{j,s}^{[BBS]}$) in our BBS observation model in part to account for correlation among data collected from the same survey route (i.e., account for routes that were consistently in better or worse habitat). Additionally, we incorporated several data filtering steps in our eBird data set to help reduce biased abundance and trend estimates associated with increased survey effort in areas with higher human activity. However, additional considerations may be needed if researchers are looking to understand population-habitat relationships⁵³.

Data integration in ecology has become common over the last 20 years as statistical theory, programming, and computing power have dramatically improved⁹. There is a growing body of literature leveraging multiple data streams to estimate species distribution, relative abundance, and population trends, including using BBS and

eBird data^{4,54,55}, Pacifici et al.²⁷ and Robinson et al.⁵⁶ showed that models with jointly analyzed data allowed for greater inference about species distributions compared to those from single dataset models. Our study provides an important example of estimating relative abundance using data collected at different spatial scales, under different observation protocols, across a gradient of bird life histories. Improvement in precision of abundance estimates provides a promising solution to traditional limitations to conservation investment, where practitioners have been limited to investing resources in places where structured surveys are available. Integrating data streams also allows for cost-effective study design, as researchers do not need to invest in only structured surveys and instead can rely on non-structured data for additional information.

We anticipate our model framework will have widespread utility, as practitioners can adjust our framework to integrate other structured datasets with publicly available, semi-structured data. Our model uses a scaling intercept and additional effort variables to scale the unstructured dataset to the scale of the structured one (informed by the known effective area of the structured survey). In many cases, practitioners may wish to integrate multiple unstructured surveys where the effective survey area is not explicitly known. While such a task is possible with our modeling structure, practitioners would need enough information about the surveys to filter for quality data (e.g., subsample data based on spatial location, temporal attributes, large differences in survey effort, etc.) and control for differences in survey effort (e.g., time of day, distance covered, time duration, etc.), thus imposing some structure on the survey data. Practitioners could then either scale one survey to another in the model or assume that, after controlling for differences in survey effort, each survey informs relative abundance on the same scale.

Integrating data from structured and semi-structured data comes with challenges. The level of model complexity required to properly integrate multiple data types and scale the data so they are comparable may be difficult for many practitioners to implement. Our modeling approach is quite intensive and may require a large amount of data for all parameters to properly converge, particularly when estimating abundance and trends in areas with low densities of study species. Additionally, community science data often requires many filtering steps to impose a “semi-structure” to ensure quality of data, which requires additional work for practitioners. Finally, while we included survey information to account for variation in detection among surveys (i.e., observer, route, survey effort), neither BBS nor eBird surveys were designed to explicitly quantify detection probabilities^{57,58}, limiting inference to relative abundance.

We encourage researchers to integrate community science data with structured surveys to improve estimates of abundance, particularly when doing so substantially increases the number of detections (e.g., areas with low densities of the species of interest or low structured survey effort, or when life history traits make a species difficult to detect). Contributions from community scientists to biological monitoring programs have the potential to increase precision of parameter estimates in a cost-effective¹ way, and we believe these benefits outweigh challenges of incorporating opportunistic or semi-structured datasets in statistical models.

Methods

Data acquisition and preparation. *Structured datasets.* We used structured North American Breeding Bird Survey (BBS) data, which is conducted annually over > 2500 routes across the United States and Canada^{11,12} during the peak of the breeding season (May and June). BBS routes were approximately 40 km long with 50 stops spaced 0.8 km apart. At each stop a 3-min point count was conducted, where all species seen or heard were recorded¹². We downloaded the entire dataset, 1966–2019, to identify each observer’s first year and account for differences in survey experience. We created a binary variable for the observers’ first year, with 1 indicating the first year they provided data, and 0 indicating all subsequent years. We then subset the data to years 2010–2019 to align with available community science data. We zero-filled BBS data by adding zeros for each species on routes in which birds were not detected in each year.

Semi-structured dataset. We used the eBird Basic Dataset as a semi-structured dataset. We used checklists within the US and Canada during June and July from 2010 to 2019. Data were filtered to impose structure on the observation process and minimize effects of unequal spatial and temporal sampling using the auk package in program R^{24,25,56,59,60}. Data were filtered to only include complete checklists where observers recorded counts of all species detected to reduce effects of preferential species reporting⁶¹. We also filtered data based on observer effort to only include checklists < 5 h in duration, < 5 km in distance travelled, and checklists with < 10 observers²⁴.

Semi-structured community science data are generally sampled unevenly across space and time. Observers tend to collect data more frequently in accessible locations close to where they live or in areas with high species diversity²⁵. Therefore, populated areas and protected areas are data rich, while expansive rural, private lands are relatively data poor. Additionally, the number of checklists submitted to eBird has increased over time. To improve spatial and temporal representation within each 1-degree grid cell block and reduce the density of checklists within populated or protected areas, we randomly sampled Canada goose data to include one detection and one non-detection checklist for each cell of a 5-km hexagonal grid in each week of June and July because of their high frequency of detections in submitted checklists²⁴. The resulting Canada goose data set consisted of 18% detections and 82% non-detections. American woodcock, black-billed cuckoo, black-throated blue warbler, loggerhead shrike, northern bobwhite and upland sandpiper were detected in < 25% of checklists submitted; there was a high proportion of non-detections compared to detections causing class imbalance. For rare species and highly imbalanced datasets, inference on species distributions may be impeded by the volume of non-detections⁶². We corrected for this class imbalance by retaining all checklists with detections and under-sampling the majority class by spatiotemporally subsampling non-detection checklists only⁶² (i.e., retaining all

checklists with detections but only one non-detection checklist for each cell of the 5-km hexagonal grid per week). Resulting datasets consisted of 1–8% detections and 92–99% non-detections.

Each eBird checklist also contained survey information to accompany the associated counts. We used survey start time, duration (in minutes), distance traveled (in km), survey type (stationary or traveling), number of observers, and a unique observer ID number for each observer to account for differences among survey data. We expected our study species to be most active and easily detected in early morning and evening. To capture activity, we converted survey start times to local solar time of day (in seconds) and calculated two continuous covariates with a 24-h period by $\cos\left(\frac{2\pi(\text{seconds})}{86400}\right)$ and $\sin\left(\frac{2\pi(\text{seconds})}{86400}\right)$, referred to as $\cos(\text{time})$ and $\sin(\text{time})$. Thus, $\cos(\text{time})$ represented night (high values) and day (low values), and $\sin(\text{time})$ represented the first half of the day (high values) and the second half of the day (low values)⁶³.

Reference grid. We overlaid a grid of 111-km \times 111-km (approximately 1° latitude \times 1° longitude near the equator) grid cells using Albers Equal Area projection across Canada and the US to estimate site-specific species relative abundance and trends. We assigned BBS routes and eBird observations to cells based on route starting points and checklist locations. We used the center points of grid cells to assign each to one of the Bird Conservation Regions (BCRs) from the North American Bird Conservation Initiative⁶⁴. We defined species ranges as all BCRs that contained grid cells where the species was observed in any dataset during our study period after removing observations of likely vagrants. We calculated the Euclidean distance of each grid cell centroid to the nearest edge of these defined ranges.

Model description. For each species, we developed two models to estimate the spatiotemporal variation of species relative abundance. The first model utilized BBS data only and the second model jointly analyzed BBS and eBird data. These models were developed under a hierarchical Bayesian framework, so they shared the same process model but had different observation or data models⁶⁵.

Process model. The process model described the trends of relative abundance by expressing relative abundance as a linear function of time (year). More specifically, we assumed that

$$\mu_{i,t}^{[\gamma]} = \alpha_{i[k]}^{[\gamma]} + \beta_{i[k]}^{[\gamma]} \times \text{YEAR}_t, \quad (1)$$

and

$$\log(\gamma_{i,t}) \sim N\left(\mu_{i,t}^{[\gamma]}, \sigma^{[\gamma]}\right), \quad (2)$$

in which $\gamma_{i,t}$ was year-specific relative abundance for grid cell i and year t , $\mu_{i,t}^{[\gamma]}$ was the mean of $\log(\gamma_{i,t})$, $\alpha_{i[k]}^{[\gamma]}$ and $\beta_{i[k]}^{[\gamma]}$ were grid cell-specific intercept and slope, respectively, for BCR k . The intercept and slope parameters, $\alpha_{i[k]}^{[\gamma]}$ and $\beta_{i[k]}^{[\gamma]}$, were random deviations from a mean intercept and slope for BCR k . For example, we had for the slope parameter ($\beta_{i[k]}^{[\gamma]}$)

$$\beta_{i[k]}^{[\gamma]} \sim N\left(\mu_{[k]}^{[\beta]}, \sigma^{[\beta]}\right), \mu_{[k]}^{[\beta]} \sim N\left(\mu^{[\beta]}, \tau^{[\beta]}\right), \quad (3)$$

in which $\mu_{[k]}^{[\beta]}$ is the BCR-specific mean of the slope parameters ($\beta_{i[k]}^{[\gamma]}$) for BCR k and $\mu^{[\beta]}$ was the grand mean of $\beta_{i[k]}^{[\gamma]}$ for all i and k . The priors for the mean parameters were assumed to be normally distributed with mean 0 and standard deviation 10 while the priors for the variance parameters were assumed to come from an inverse gamma distribution with shape and rate parameters 0.01. In this way we allowed the intercept and slope parameters to vary across any grid cell, but also assumed that grid cells within the same BCR have more similar values than grid cells in different BCRs⁶⁶. This allowed us to additionally estimate relative abundance and relative abundance trends in grid cells without any count data based on these relationships among grid cells in the same BCR. We used the same model for the grid cell-specific intercepts ($\alpha_{i[k]}^{[\gamma]}$) with an intercept grand mean $\mu^{[\alpha]}$, BCR-specific mean $\mu_{[k]}^{[\alpha]}$, and variance parameters $\sigma^{[\alpha]}$ and $\tau^{[\alpha]}$, assuming the same priors.

Note that we centered YEAR_t so that the middle year (i.e., between 2014 and 2015 for our 2010–2019 study period) was 0. Thus $\exp\left(\alpha_{i[k]}^{[\gamma]}\right)$ was the mean relative abundance for grid cell i across the study period, and $\beta_{i[k]}^{[\gamma]}$ the grid cell-specific trend of log relative abundance during the study period. We used Eq. (2) to add additional Gaussian noise to our mean log relative abundance estimates, $\mu_{i,t}^{[\gamma]}$, to account for overdispersion in year-specific relative abundance, $\gamma_{i,t}$, in grid cell i in year t . We assumed the variance parameter $\sigma^{[\gamma]}$ came from an inverse gamma distribution with shape and rate parameters 0.01.

Observation model (BBS model). We hierarchically linked year-specific relative abundance (γ), and by extension, mean relative abundance (α) and relative abundance trends (β), from the process model to BBS count data ($y^{[BBS]}$). Because BBS data contained a larger proportion of non-detections (0 counts) than predicted with a Poisson distribution (as determined by posterior predictive checks), we assumed that data were generated from a zero-inflated Poisson process such that

$$y_{j,s,i,t}^{[BBS]} \sim \text{Poisson}\left[\lambda_{j,s,i,t}^{[BBS]} \times \left(1 - z_{j,s,i,t}^{[BBS]}\right)\right], \quad (4)$$

in which $y_{j,s,i,t}^{[BBS]}$ was the BBS count for route j (sum of counts across all 50 stops) surveyed by observer s in grid cell i and year t , $\lambda_{j,s,i,t}^{[BBS]}$ was the expectation of count data $y_{j,s,i,t}^{[BBS]}$, and $z_{j,s,i,t}^{[BBS]}$ was a Bernoulli random variable with probability $\omega^{[BBS]}$, where $\omega^{[BBS]} \sim U(0, 1)$.

To achieve grid cell-level inference, we offset the grid cell relative abundance by the effective area surveyed by BBS routes to scale the grid cell relative abundance to BBS route-level relative abundance. More specifically, we assumed

$$\log\left(\lambda_{j,s,i,t}^{[BBS]}\right) = \log\left(\gamma_{i,t} \times (25/12,321)\right) + \varepsilon_{j,s}^{[BBS]} + \eta^{[BBS]} \times I_{j,s,t}^{[BBS]}, \quad (5)$$

where 25/12,321 was the effective area surveyed by a BBS route ($\sim 25 \text{ km}^2$; 50 stops each with a 400 m survey radius¹²) divided by the area of a single grid cell (12,321 km^2). To account for detection error related to observer experience, we included $\varepsilon_{j,s}^{[BBS]}$ as a route- and observer-specific error term, and $\eta^{[BBS]}$ as an additional term of observation error if route j was surveyed by a first-time observer s ^{12,67} (indicated by $I_{j,s,t}^{[BBS]}$). We assumed $\varepsilon_{j,s}^{[BBS]}$ was normally distributed with mean 0 and variance $\sigma^{[BBS]}$, where $\sigma^{[BBS]}$ came from an inverse gamma distribution with shape and rate parameters 0.01. We assumed $\eta^{[BBS]}$ was normally distributed with a mean 0 and standard deviation 10.

Observation model (joint model). In the joint model, we again linked year-specific relative abundance (γ) from the process model to BBS count data using Eqs. (4) and (5). Similarly, we hierarchically linked year-specific relative abundance to eBird count data ($y^{[eBird]}$). Thus, both datasets informed year-specific relative abundance (γ), mean relative abundance (α) and relative abundance trend (β) estimates. We again used a zero-inflated Poisson distribution such that

$$y_{j,s,i,t}^{[eBird]} \sim \text{Poisson}\left[\lambda_{j,s,i,t}^{[eBird]} \times \left(1 - z_{j,s,i,t}^{[eBird]}\right)\right], \quad (6)$$

in which $y_{j,s,i,t}^{[eBird]}$ was the eBird count for checklist j surveyed by observer s in grid cell i and year t , $\lambda_{j,s,i,t}^{[eBird]}$ was the expected count, and $z_{j,s,i,t}^{[eBird]}$ was a Bernoulli random variable with probability $\omega^{[eBird]}$, where $\omega^{[eBird]} \sim U(0, 1)$.

For eBird data, we again considered the variation among checklists. Instead of observer experience, we considered additional survey effort variables that potentially influenced the distribution of counts. We assumed

$$\begin{aligned} \log\left(\lambda_{j,s,i,t}^{[eBird]}\right) = & \log\left(\gamma_{i,t}\right) + \beta_0^{[eBird]} + \beta_1^{[eBird]} \times \text{TYPE}_{j,s,i,t} + \beta_2^{[eBird]} \times \text{DIST}_{j,s,i,t} + \beta_3^{[eBird]} \times \text{COSTIME}_{j,s,i,t} \\ & + \beta_4^{[eBird]} \times \text{SINTIME}_{j,s,i,t} + \beta_5^{[eBird]} \times \text{DURA}_{j,s,i,t} + \beta_6^{[eBird]} \times \text{NOOB}_{j,s,i,t} + \varepsilon_s^{[eBird]}, \end{aligned} \quad (7)$$

in which $\text{TYPE}_{j,s,i,t}$ was survey type (i.e., 1 for point count and 0 for transect), $\text{DIST}_{j,s,i,t}$ was survey distance, $\text{COSTIME}_{j,s,i,t}$ and $\text{SINTIME}_{j,s,i,t}$ were cos(time) and sin(time), respectively, of start times of the survey, $\text{DURA}_{j,s,i,t}$ was the survey duration, and $\text{NOOB}_{j,s,i,t}$ was the number of observers. We included $\varepsilon_s^{[eBird]}$ as an observer-specific error term to account for correlation among counts from the same observer. We were unable to calculate the effective area surveyed for individual eBird checklists. Instead, we included $\beta_0^{[eBird]}$, an additional scaling intercept to relate eBird relative abundance estimates from the checklist level to the grid cell level. We assumed $\beta_{0-6}^{[eBird]}$ were normally distributed with mean 0 and standard deviation 10. We assumed $\varepsilon_s^{[eBird]}$ was normally distributed with mean 0 and variance $\sigma^{[eBird]}$, where $\sigma^{[eBird]}$ came from an inverse gamma distribution with shape and rate parameters 0.01.

Additional considerations to improve model convergence. We further altered American woodcock and Canada goose joint models to improve model convergence. The BBS and eBird datasets contained fewer detections of American woodcocks than in other species; thus, we predicted that model convergence issues in the American woodcock models were due to lack of sufficient data across BBS and eBird datasets. To increase our data sample sizes, we used data from the American woodcock Singing Ground Survey (SGS) as a third data source for American woodcock models (see Supplementary Information). The American woodcock SGS is specifically designed for detecting this cryptic species, so detectability is likely higher during this survey compared to surveys not specifically designed for American woodcocks. We developed another model to jointly analyze BBS, eBird, and SGS datasets (see Supplementary Information). This model used the same process model, BBS observation model, and eBird observation model described in Eqs. (1)–(7).

Canada geese frequently form large flocks (often 100 s or 1000 s of individuals), a unique ecological trait among our study species. Thus, both BBS and eBird Canada goose data contained uniquely high counts among our data (max counts of 2900 and 3000 Canada geese in BBS and eBird data, respectively). We predicted that convergence issues in the Canada goose joint model were due to overdispersion resulting from uniquely high counts, especially in the eBird data where these counts were more frequent than in the BBS data. To account for this overdispersion, we added additional Gaussian noise to $\lambda_{j,s,i,t}^{[eBird]}$ in Eq. (7) (see Supplementary Information).

Model implementation. We used Markov Chain Monte Carlo and a Gibbs sampler in JAGS⁶⁸ using the jagsUI package⁶⁹ in program R⁶¹. We ran at minimum 9000 iterations, discarded at minimum the first 5000 samples as burn-in, and retained at least 4000 samples with no thinning from 3 chains (exact number of iterations needed to achieve convergence varied among models). We evaluated convergence using the Gelman–Rubin statistic⁷⁰ ($\hat{R} < 1.2$) and visual assessments of traceplots. We used a modified CV calculation to assess improve-

ments in precision for α , γ , and β (i.e., mean relative abundance, year-specific relative abundance, and trend estimates, respectively) parameters between BBS and joint models. For α and γ parameters,

$$\begin{aligned} CV^{[\alpha]} &= \left(\widehat{\alpha}_{(0.975)} - \widehat{\alpha}_{(0.025)} \right) / \left| \widehat{\alpha}_{(0.5)} \right|, \\ CV^{[\gamma]} &= \left(\widehat{\gamma}_{(0.975)} - \widehat{\gamma}_{(0.025)} \right) / \left| \widehat{\gamma}_{(0.5)} \right|, \end{aligned} \quad (8)$$

and for β

$$CV^{[\beta]} = \left(\widehat{\beta}_{(0.975)} - \widehat{\beta}_{(0.025)} \right), \quad (9)$$

where $\widehat{\alpha}_{(p)}$, $\widehat{\gamma}_{(p)}$, and $\widehat{\beta}_{(p)}$ are the p th quantiles of the posterior distribution for α , γ , and β , respectively. Smaller CVs indicated more precise estimates of comparable parameters. We calculated CVs of each parameter for each grid cell. We subtracted the joint model CVs for each parameter for each grid cell from corresponding BBS-only model CVs to evaluate the magnitude of improvement in precision for each grid cell and evaluated overall improvements for each parameter by calculating the proportion of grid cells for which joint model CVs < corresponding BBS-only model CVs.

Data availability

All data used in this manuscript are publicly available through eBird (Cornell Lab of Ornithology, National Audubon Society), North American Breeding Bird Survey (United States Geological Survey, Environment & Climate Change Canada), and American Woodcock Singing Ground Survey (United States Fish & Wildlife Service).

Received: 8 November 2021; Accepted: 2 November 2022

Published online: 24 November 2022

References

- Dickinson, J. L., Zuckerberg, B. & Bonter, D. N. Citizen science as an ecological research tool: Challenges and benefits. *Annu. Rev. Ecol. Evol. Syst.* **41**, 149–172 (2010).
- Tulloch, A. I. T., Possingham, H. P., Joseph, L. N., Szabo, J. & Martin, T. G. Realising the full potential of citizen science monitoring programs. *Biol. Conserv.* **165**, 128–138 (2013).
- McKinley, D. C. *et al.* Citizen science can improve conservation science, natural resource management, and environmental protection. *Biol. Conserv.* **208**, 15–28 (2017).
- Isaac, N. J. B. *et al.* Data integration for large-scale models of species distributions. *Trends Ecol. Evol.* **35**, 56–67 (2020).
- Hochachka, W. M. *et al.* Data-intensive science applied to broad-scale citizen science. *Trends Ecol. Evol.* **27**, 130–137 (2012).
- Fink, D. *et al.* Modeling avian full annual cycle distribution and population trends with citizen science data. *Ecol. Appl.* **30**, e02056. <https://doi.org/10.1002/eap.2056> (2020).
- Miller, D. A. W., Pacifici, K., Sanderlin, J. S. & Reich, B. J. The recent past and promising future for data integration methods to estimate species' distributions. *Methods Ecol. Evol.* **10**, 22–37 (2019).
- Koshkina, V. *et al.* Integrated species distribution models: combining presence-background data and site-occupancy data with imperfect detection. *Methods Ecol. Evol.* **8**, 420–430 (2017).
- Zipkin, E. F. *et al.* Addressing data integration challenges to link ecological processes across scales. *Front. Ecol. Environ.* **19**, 30–38 (2021).
- Sun, C. C., Royle, J. A. & Fuller, A. K. Incorporating citizen science data in spatially explicit integrated population models. *Ecology* **100**, e02777. <https://doi.org/10.1002/ecy.2777> (2019).
- Pardieck, K. L., Ziolkowski, D. J., Lutmerding, M., Aponte, V. I. & Hudson, M.-A. R. *North American Breeding Bird Survey Dataset 1966–2019: U.S. Geological Survey Data Release*. <https://doi.org/10.5066/P9J6QUF6> (2020). Accessed 1 June 2020.
- Sauer, J. R. & Link, W. A. Analysis of the North American breeding bird survey using hierarchical models. *Auk* **128**, 87–98 (2011).
- Horns, J. J., Adler, F. R. & Şekercioğlu, Ç. H. Using opportunistic citizen science data to estimate avian population trends. *Biol. Conserv.* **221**, 151–159 (2018).
- Walker, J. & Taylor, P. D. Evaluating the efficacy of ebird data for modeling historical population trajectories of North American birds and for monitoring populations of boreal and arctic breeding species. *Avian Conserv. Ecol.* **15**, 10. <https://doi.org/10.5751/ACE-01671-150210> (2020).
- Betts, M. G., Mitchell, D., Diamond, A. W. & Bety, J. Uneven rates of landscape change as a source of bias in roadside wildlife surveys. *J. Wildl. Manag.* **71**, 2266–2273 (2007).
- Harris, J. B. C. & Haskell, D. G. Land cover sampling biases associated with roadside bird surveys bias. *Avian Conserv. Ecol.* **2**, 12 (2007).
- Wellcome, T. I., Kardynal, K. J., Franken, R. J. & Gillies, C. S. Off-road sampling reveals a different grassland bird community than roadside sampling: Implications for survey design and estimates to guide conservation. *Avian Conserv. Ecol.* **9**, 4. <https://doi.org/10.5751/ace-00624-090104> (2014).
- Weiser, E. L., Diffendorfer, J. E., Lopez-Hoffman, L., Semmens, D. & Thogmartin, W. E. Challenges for leveraging citizen science to support statistically robust monitoring programs. *Biol. Conserv.* **242**, 108411. <https://doi.org/10.1016/j.biocon.2020.108411> (2020).
- Kelling, S. *et al.* Using semistructured surveys to improve citizen science data for monitoring biodiversity. *Bioscience* **69**, 170–179 (2019).
- Sullivan, B. L. *et al.* eBird: A citizen-based bird observation network in the biological sciences. *Biol. Conserv.* **142**, 2282–2292 (2009).
- Clark, C. J. eBird records show substantial growth of the Allen's Hummingbird (*Selasphorus sasin sedentarius*) population in urban Southern California. *Condor* **119**, 122–130 (2017).
- Zuckerberg, B., Fink, D., la Sorte, F. A., Hochachka, W. M. & Kelling, S. Novel seasonal land cover associations for eastern North American forest birds identified through dynamic species distribution modelling. *Divers. Distrib.* **22**, 717–730 (2016).
- Robinson, O. J. *et al.* Using citizen science data in integrated population models to inform conservation. *Biol. Conserv.* **227**, 361–368 (2018).
- Strimas-Mackey, M. *et al.* *Best Practices for Using eBird Data* (Cornell Lab of Ornithology, 2020).
- Johnston, A. *et al.* Analytical guidelines to increase the value of community science data: An example using eBird data to estimate species distributions. *Divers. Distrib.* **27**, 1265–1277 (2021).

26. Dorazio, R. M. Accounting for imperfect detection and survey bias in statistical analysis of presence-only data. *Glob. Ecol. Biogeogr.* **23**, 1472–1484 (2014).
27. Pacifici, K. *et al.* Integrating multiple data sources in species distribution modeling: A framework for data fusion. *Ecology* **98**, 840–850 (2017).
28. Rosenberg, K. V., Blancher, P. J., Stanton, J. C. & Panjabi, A. O. Use of North American breeding bird survey data in avian conservation assessments. *Condor* **119**, 594–606 (2017).
29. Boersch-Supan, P. H., Trask, A. E. & Baillie, S. R. Robustness of simple avian population trend models for semi-structured citizen science data is species-dependent. *Biol. Conserv.* **240**, 108286. <https://doi.org/10.1016/j.biocon.2019.108286> (2019).
30. McAuley, D. G., Keppie, D. M. & Whiting, R. M. American woodcock (*Scolopax minor*). In *Birds of the World* (ed. Poole, A. F.) (Cornell Lab of Ornithology, 2020).
31. Hughes, J. M. Black-billed cuckoo (*Coccyzus erythrophthalmus*). In *Birds of the World* (ed. Rodewald, P. G.) (Cornell Lab of Ornithology, 2020).
32. Holmes, R. T. *et al.* Black-throated blue warbler (*Setophaga caerulescens*). In *Birds of the World* (ed. Rodewald, P. G.) (Cornell Lab of Ornithology, 2020).
33. Mowbray, T. B., Ely, C. R., Sedinger, J. S. & Trost, R. E. Canada goose (*Branta canadensis*). In *Birds of the World* (ed. Rodewald, P. G.) (Cornell Lab of Ornithology, 2020).
34. Houston, C. S., Jackson, C. & Bowen, D. E. Upland sandpiper (*Bartramia longicauda*). In *Birds of the World* (ed. Poole, A. F.) (Cornell Lab of Ornithology, 2020).
35. Yosef, R. Loggerhead shrike (*Lanius ludovicianus*). In *Birds of the World* (eds Poole, A. F. & Gill, F. B.) (Cornell Lab of Ornithology, 2020).
36. Brennan, L. A., Hernandez, F. & Williford, D. Northern bobwhite (*Colinus virginianus*). In *Birds of the World* (ed. Poole, A. F.) (Cornell Lab of Ornithology, 2020).
37. Couturier, T., Cheylan, M., Bertolero, A., Astruc, G. & Besnard, A. Estimating abundance and population trends when detection is low and highly variable: A comparison of three methods for the Hermann's tortoise. *J. Wildl. Manag.* **77**, 454–462 (2013).
38. Johnson, D. H. In defense of indices: The case of bird surveys. *J. Wildl. Manag.* **72**(4), 857–868 (2008).
39. Johnston, A. *et al.* Abundance models improve spatial and temporal prioritization of conservation resources. *Ecol. Appl.* **25**(7), 1749–1756 (2015).
40. Rosenberg, K. V., Blancher, P. J., Stanton, J. C. & Panjabi, A. O. Use of North American breeding bird survey data in avian conservation assessments. *Condor* **119**(3), 594–606 (2017).
41. Niven, D., Sauer, J., Butcher, G. & Link, W. Christmas bird count provides insights into population change in land birds that breed in the boreal forest. *Am. Birds* **58**, 10–20 (2004).
42. Roy, C. *et al.* Monitoring boreal avian populations: How can we estimate trends and trajectories from noisy data? *Avian Conserv. Ecol.* **14**, 8. <https://doi.org/10.5751/ACE-01397-140208> (2019).
43. Robbins, C. S., Dawson, D. K. & Dowell, B. A. Habitat area requirements of breeding forest birds of the middle Atlantic states. *Wildlife Monogr.* **103**, 1–34 (1989).
44. Yip, D. A., Bayne, E. M., Sólomos, P., Campbell, J. & Proppe, D. Sound attenuation in forest and roadside environments: Implications for avian point-count surveys. *Condor* **119**, 73–84 (2017).
45. Zhang, G. Spatial and temporal patterns in volunteer data contribution activities: A case study of eBird. *ISPRS Int. J. Geo-Inf.* **9**, 597. <https://doi.org/10.3390/ijgi9100597> (2020).
46. Johnson, C. A. *Detection, Habitat Use, and Occupancy Dynamics of Black-Billed Cuckoos and Yellow-Billed Cuckoos in Illinois*. University of Illinois Urbana-Champaign, Thesis (2021).
47. Sauer, J. R., Link, W. A., Kendall, W. L., Kelley, J. R. & Niven, D. K. A hierarchical model for estimating change in American woodcock populations. *J. Wildl. Manag.* **72**(10), 204–214 (2008).
48. Maguire, B. Niche response structure and the analytical potentials of its relationship to the habitat. *Am. Nat.* **107**, 213–246 (1973).
49. Martínez-Meyer, E., Díaz-Porras, D., Peterson, A. T. & Yáñez-Arenas, C. Ecological niche structure and rangewide abundance patterns of species. *Biol. Lett.* **9**, 20120637 (2013).
50. Osorio-Olvera, L., Yáñez-Arenas, C., Martínez-Meyer, E. & Peterson, A. T. Relationships between population densities and niche-centroid distances in North American birds. *Ecol. Lett.* **23**, 555–564 (2020).
51. Manthey, J. D. *et al.* A test of niche centrality as a determinant of population trends and conservation status in threatened and endangered North American birds. *Endanger. Species Res.* **26**, 201–208 (2015).
52. Jones, J. P. G. Monitoring species abundance and distribution at the landscape scale. *J. Appl. Ecol.* **48**, 9–13 (2011).
53. van der Burg, M. P., Bly, B., VerCauteren, T. & Tyre, A. J. Making better sense of low density species using a spatially explicit modelling approach. *J. Appl. Ecol.* **48**, 47–55 (2011).
54. Fletcher, R. J. *et al.* A practical guide for combining data to model species distributions. *Ecology* **100**, e02710. <https://doi.org/10.1002/ecy.2710> (2019).
55. Knight, E. C., Smith, A. C., Brigham, R. M. & Bayne, E. M. Combination of targeted monitoring and breeding bird survey data improves population trend estimation and species distribution modeling for the Common Nighthawk. *Ornithol. Appl.* **123**, 005. <https://doi.org/10.1093/ornithapp/duab005> (2021).
56. Robinson, O. J. *et al.* Integrating citizen science data with expert surveys increases accuracy and spatial extent of species distribution models. *Divers. Distrib.* **26**, 976–986 (2020).
57. Campbell, M. & Francis, C. M. Using stereo-microphones to evaluate observer variation in North American breeding bird survey point counts. *Auk* **128**, 303–312 (2011).
58. Twedt, D. J. Estimating regional landbird populations from enhanced North American breeding bird surveys. *J. Field Ornithol.* **86**, 352–368 (2015).
59. Strimas-Mackey, M., Miller, E. & Hochachka, W. *Auk: eBird Data Extraction and Processing with AWK. R Package. Version 0.3.0*. <https://cornelllabofornithology.github.io/auk/> (2018). Accessed 1 June 2020.
60. R Core Team. *R: A Language and Environment for Statistical Computing* (R Foundation for Statistical Computing, 2020).
61. Troudet, J., Grandcolas, P., Blin, A., Vignes-Lebbe, R. & Legendre, F. Taxonomic bias in biodiversity data and societal preferences. *Sci. Rep.* **7**, 9132. <https://doi.org/10.1038/s41598-017-09084-6> (2017).
62. Robinson, O. J., Ruiz-Gutierrez, V. & Fink, D. Correcting for bias in distribution modelling for rare species using citizen science data. *Divers. Distrib.* **24**, 460–472 (2018).
63. Schafer, T. L. J., Wikle, C. K., VonBank, J. A., Ballard, B. M. & Weegman, M. D. A Bayesian Markov Model with Pólya-Gamma sampling for estimating individual behavior transition probabilities from accelerometer classifications. *J. Agric. Biol. Environ. Stat.* **25**, 365–382 (2020).
64. Bird Studies Canada & NABCI. *Bird Conservation Regions*. <https://www.birdscanada.org/bird-science/nabci-bird-conservation-regions/> (2014).
65. Berliner, L. M. Hierarchical Bayesian time series models. In *Maximum Entropy and Bayesian Methods* (eds Hanson, K. M. & Silver, R. N.) 15–22 (Springer, 1996).
66. Zhao, Q., Boomer, G. S. & Royle, J. A. Integrated modeling predicts shifts in waterbird population dynamics under climate change. *Ecography* **42**, 1470–1481 (2019).

67. Bled, F., Sauer, J., Pardieck, K., Doherty, P. & Royle, J. A. Modeling trends from North American breeding bird survey data: A spatially explicit approach. *PLoS ONE* **8**, e81867. <https://doi.org/10.1371/journal.pone.0081867> (2013).
68. Plummer, M. *et al.* JAGS: A program for analysis of Bayesian graphical models using Gibbs sampling. In *Proc. 3rd Int. Work. Distrib. Stat. Comput.*, Vol. 124, 1–10 (2003).
69. Kellner, K. jagsUI: A wrapper around “rjags” to streamline “JAGS” analyses. *R Package. Version 1.5.1*. <https://CRAN.R-project.org/package=jagsUI> (2019). Accessed 1 June 2020.
70. Brooks, S. P. & Gelman, A. General methods for monitoring convergence of iterative simulations. *J. Comput. Graph. Stat.* **7**, 434–455 (1998).

Acknowledgements

The authors thank the thousands of observers who recorded birds during the North American Breeding Bird Survey, American Woodcock Singing Ground Survey and via submitted checklists on eBird.org. They thank Jay VonBank for discussions about analyses and plotting. They also thank their employers for supporting this work.

Author contributions

A.R.S., T.L.J.S., S.A.C., E.A.S., S.J.C., F.M.D., A.R.M., M.D.W., and Q.Z. conceived the study. S.A.C., E.A.S., and F.M.D. compiled and prepared the data. A.R.S., T.L.J.S., Q.Z. designed the statistical methods with input from S.A.C., E.A.S., S.J.C., F.M.D., A.R.M., and M.D.W. A.R.S., T.L.J.S., E.A.S., and S.J.C. performed the analyses. A.R.S., S.A.C., E.A.S., S.J.C., and M.D.W. led the writing of the manuscript. C.M.W. and A.A.S. contributed to data interpretation. A.R.S. and S.A.C. produced the figures. All authors edited the manuscript and contributed to revisions. M.D.W. and Q.Z. oversaw the project. All authors reviewed the manuscript and approved the final draft.

Competing interests

The authors declare no competing interests.

Additional information

Supplementary Information The online version contains supplementary material available at <https://doi.org/10.1038/s41598-022-23603-0>.

Correspondence and requests for materials should be addressed to A.R.S.

Reprints and permissions information is available at www.nature.com/reprints.

Publisher's note Springer Nature remains neutral with regard to jurisdictional claims in published maps and institutional affiliations.



Open Access This article is licensed under a Creative Commons Attribution 4.0 International License, which permits use, sharing, adaptation, distribution and reproduction in any medium or format, as long as you give appropriate credit to the original author(s) and the source, provide a link to the Creative Commons licence, and indicate if changes were made. The images or other third party material in this article are included in the article's Creative Commons licence, unless indicated otherwise in a credit line to the material. If material is not included in the article's Creative Commons licence and your intended use is not permitted by statutory regulation or exceeds the permitted use, you will need to obtain permission directly from the copyright holder. To view a copy of this licence, visit <http://creativecommons.org/licenses/by/4.0/>.

© The Author(s) 2022